RSC Advances

PAPER

View Article Online
View Journal | View Issue

Cite this: *RSC Adv.*, 2016, **6**, 10233

Triple-shape memory effects of bismaleimide based thermosetting polymer networks prepared *via* heterogeneous crosslinking structures

Qiwei Zhang,[a] Hongqiu Wei,[a] Yanju Liu,[b] Jinsong Leng*[a] and Shanyi Du[a]

Received 16th November 2015
Accepted 15th January 2016

DOI: 10.1039/c5ra24247a

www.rsc.org/advances

Functional physical behavior, including triple shape memory process and reversible actuation, has attracted great interest in the research field of thermosetting polymers in recent years. Herein, we synthesized a series of covalent crosslinking thermosetting polymers with triple shape memory effects *via* introducing bisphenol-A cyanate ester (BACE) to bismaleimide (BMI) networks. Due to the complex covalent crosslinking structures, such BMI based triple-shape memory polymers (TSMPs) present broad glass transition temperature ranges, which is a crucial precondition for the triple-shape memory behavior. Results demonstrated that BMI based TSMPs showed excellent thermal stabilities and mechanical properties. Moreover, triple shape memory behavior was achieved successfully by choosing two switching temperatures to fix two separate shapes independently. Upon heating, both the programmed shapes could recover to their former shape separately. This paper provides fundamental attempts for the further development of thermosetting triple shape memory polymers. Combining the superior comprehensive properties with the smart triple shape memory behavior, such materials present great potential to be applied as smart materials and structures, especially for aerospace areas.

Introduction

Shape memory polymers (SMPs) are a class of polymeric materials that present the ability of being deformed to a temporary shape and not recovering to their initial shape until they are stimulated by some external influencing factors[1,2] such as temperature,[3] light,[4] electric or magnetic fields,[5] solvent,[6] pH value[7] and even enzymes.[8] Investigating the relationship between chemical structure and crucial properties, SMPs have their original shapes because of physical or chemical crosslinking. The materials can be changed to temporary shapes by applying external force when the samples are heated over a critical transition temperature (T_t). Such temporary shapes can be fixed at a temperature lower than T_t due to the freezing of polymer chains.[9] The shape recovery of SMPs, which results from polymer chain segments relaxation, can be observed during the reheating process under stress-free conditions. Based on such a unique smart capability, SMPs have contributed to various areas such as biomedical devices,[10] sensors,[11] actuators,[12] smart textiles[13] and deployable space structures.[14]

Thermosetting SMPs structurally consist of covalently crosslinked amorphous networks. They are a class of materials with attractive features like high reliability and excellent shape memory properties.[15–17] Compared with thermoplastic semi-crystalline SMPs, thermosetting SMPs have a consistent performance during the glass transition process and flexible properties in the elastomeric state.[18] It depends on the permanent covalent crosslinked network thermosetting SMPs possessed. This type of SMPs also display high shape recovery ratio with quick response, tunable work capacity during recovery and good shape fixity due to suppression of creep.[19–21] The permanent shapes of thermosetting SMPs will be obtained once the covalent crosslinked networks are formed during initial processing. The magnitude of deformations or the temporary deformed shape cannot affect the shape memory effect of these materials.

The SMPs only can have a dual shape memory effect. In recent years, there are a large number of SMPs with new properties emerging with urgent requirements of extending both the practical and potential applications. Multiple shape memory polymers, which have the capability of memorizing three or more shapes during the shape changing and recovery process, have been investigated systematically. To date, many types of research about thermoplastic multiple shape polymeric systems have been reported.[22–24] However, the investigation of multiple shape memory effect of thermosetting polymers is far inadequate. Mather *et al.* blended epoxy and poly (ε-caprolactone) as a simple route of producing a triple shape memory composite.[25,26] This method utilized the requisite combination of microstructure and composition to achieve triple-shape memory effect that formed by polymerization-induced phase separation. Xie *et al.* reported

[a]*Center for Composite Materials and Structures, Harbin Institute of Technology (HIT), Harbin 150080, People's Republic of China. E-mail: lengjs@hit.edu.cn; Fax: +86-451-86402328; Tel: +86-451-86402328*

[b]*Department of Astronautical Science and Mechanics, Harbin Institute of Technology (HIT), Harbin 150080, People's Republic of China*

a polymer bilayer structure consisting of thermosetting epoxy with two different glass transition temperatures (T_g).[27] By changing the ratio of the thickness of the two layers, the shape memory properties could be tuned easily. Moreover, Li *et al.*[28,29] observed a weak triple shape memory effect on thermoset shape memory polymer with narrow glass transition. Cold compression programming as a time and energy efficient approach for thermoset polymer was discussed. However, thermosetting triple-shape memory polymers obtained by previous approaches could not be used as high-performance matrix resins of advanced composites directly and conveniently. To overcome this drawback, it is necessary to fabricate thermosetting polymers with intrinsic multiple shape memory effect.

Bismaleimide (BMI) resin as thermosetting polymer matrix possessed a better performance than typical phenolics and epoxies at high temperature.[30] SMPs based on BMI resin with dual-shape memory behavior and tunable transition temperatures have been investigated by Air Force Research Laboratory in previous reports, which shows a great potential to be applied in the fields of morphing structures and deployable structures.[31] For further develop and enhance the intelligence of BMI based SMPs to meet the practical and smart applications, we synthesized a series of BMI based TSMPs with triple shape memory effect by introducing bisphenol-A cyanate ester (BACE) into the polymeric system as a kind of crosslinking agent. Unlike other reported physical approaches, this chemical crosslinking method had little adverse effect on the integral performance of the materials we synthesized. We further revealed that the broad T_g range of BMI based TSMPs contributed to the triple shape memory behavior. The thermal and mechanical properties affected by the crosslink density are discussed in detail. The dual and triple shape memory effects, caused by complex covalent crosslinks, are characterized in both tensile tests and bending tests.

Experimental section

Materials synthesis

4,4′-Bismaleimidodiphenylmethane (BDM) and 2,2′-bis(4-cyanatophenyl)propane (BACE) were purchased from Tokyo Chemical Industry CO., LTD. A polyether diamine, poly-(propylene glycol) bis(2-aminopropyl ether) (D400) (M_w = 400 g mol^{-1}), was purchased from Aladdin. The chemical structures of BDM, D400 and BACE were depicted in Fig. 1a–c, respectively. All chemicals were analytic grade and used as received without further purification.

The whole synthetic process shown in Fig. 1d could be separated into two steps as follows. First, BDM was reacted with D400 to build the linear backbone of the molecular structure by following a reported method.[32] In brief, the reaction was carried out in a three-neck flask equipped with a mechanical stirrer, a condenser tube, and argon atmosphere. A calculated amount of BDM and D400 were mixed in tetrahydrofuran (THF) with stirring at the temperature of 65 °C for 24 h under argon. The molecular weight and its distribution for the backbone polymer had been tested by gel permeation chromatography (GPC; Agilent 1100). The weight-average molecular weight (M_w) of linear polymer backbone was 27 830 and the polydispersity index (M_w/M_n) was about 2.0. The bright yellow coloured solution became viscous amber colored one after the process above. Second, after filtering the solution to remove any particles, the weighed BACE was added to the solution depending on the ratios shown in Table 1. The mixture was stirred rapidly for another 5 min to

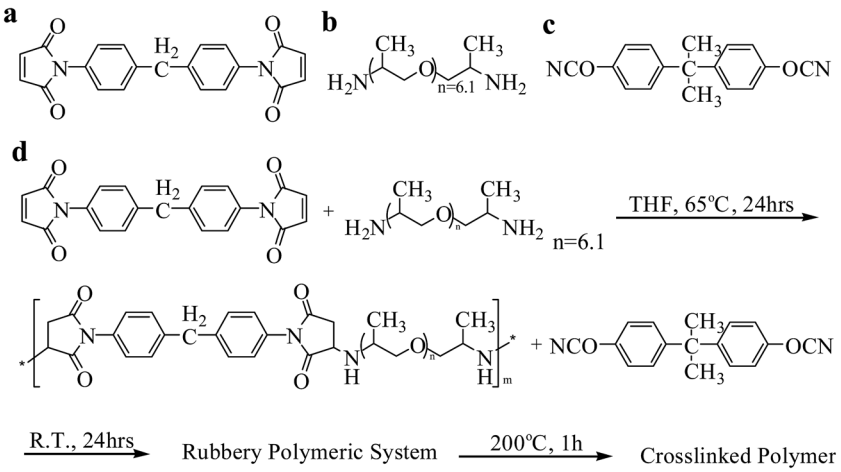

Fig. 1 The chemical structures of (a) 4,4′-bismaleimidodiphenylmethane (BDM), (b) D400, and (c) 2,2′-bis(4-cyanatophenyl)propane (BACE) for (d) preparation of BMI based TSMPs.

Table 1 Details of BMI based TSMPs synthesis

Sample no.	TSMP1	TSMP2	TSMP3	TSMP4
Mole fraction of BDM/JA-400/BACE	1/1/0.25	1/1/0.5	1/1/0.75	1/1/1
BACE to BDM mass ratio (%)	19.4	38.8	58.2	77.7

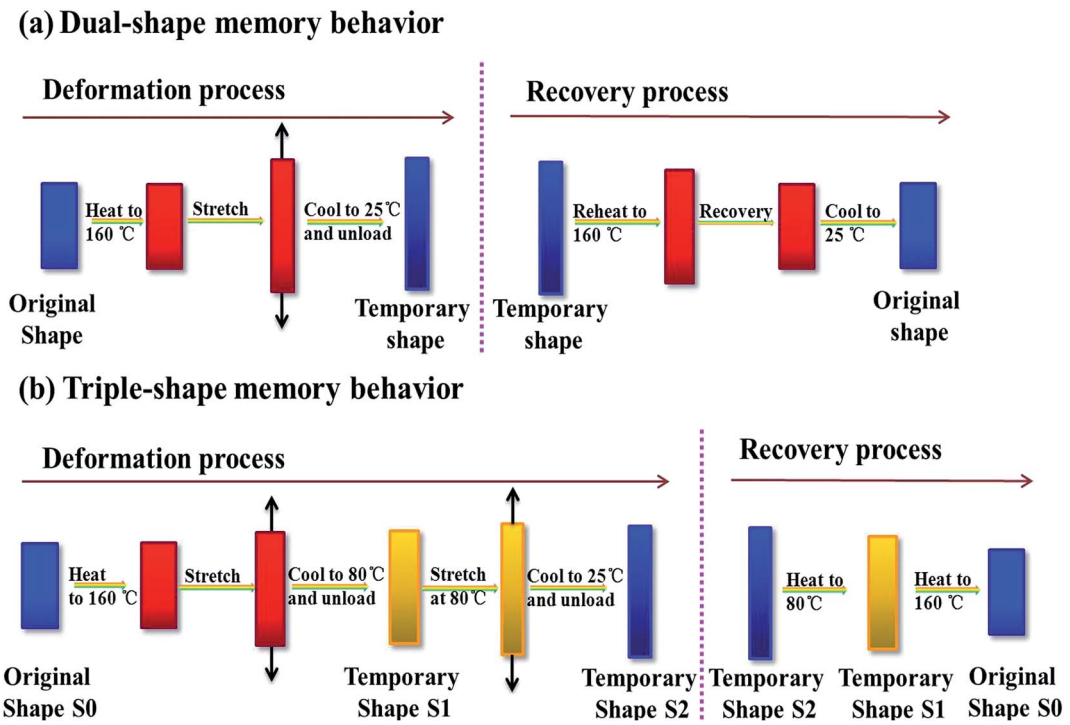

Fig. 2 Schematic description of (a) dual-shape memory testing and (b) triple-shape memory testing.

obtain a homogeneous solution. The resulting viscous solution was cast into a mould covered by a release layer and dried over for 24 h at room temperature. The resulting rubbery polymeric system was thermally cured at 200 °C for one hour. Finally, a series of BMI based TSMPs samples containing different crosslinking density were fabricated by adjusting the amount of BACE.

Characterization

FTIR spectra, which was used to investigate the variations of the chemical structures, was recorded on a spectrum (Perkin-Elmer, MA, USA) with the accessory of universal attenuated total refraction (ATR), which the wavenumbers coverage is from 4000 cm^{-1} to 650 cm^{-1} with a resolution of 4 cm^{-1}.

Thermogravimetric analysis (TGA) was carried out by Mettler-Toledo thermal analysis instrument (TGA/DSC1 SF1942). The data was collected from 25 °C to 600 °C at a heating rate of 10 °C min^{-1} under nitrogen atmosphere. Differential scanning calorimetry (DSC, Mettler-Toledo DSC1) measurements were used to characterize the change in the thermal properties of the polymers from 40 °C to 160 °C at a heating rate of 10 °C min^{-1}. The glass transition temperature (T_g) values were obtained as the inflection temperatures in the DSC curves.

Thermal-mechanical properties were investigated by dynamic mechanical analysis (DMA, SDTA861e Mettler Toledo) under a tensile mode. The storage modulus and loss factors of the samples obtained from this test were crucial for SMPs. The samples with dimension of 25 × 3 × 1 mm^3 were heated from 25 °C to 200 °C at a rate of 2 °C min^{-1} and a frequency of 1 Hz.

The static mechanical properties were conducted by a tensile test on Zwick/Roell Z010 (Zwick GmbH & Co. KG) instrument

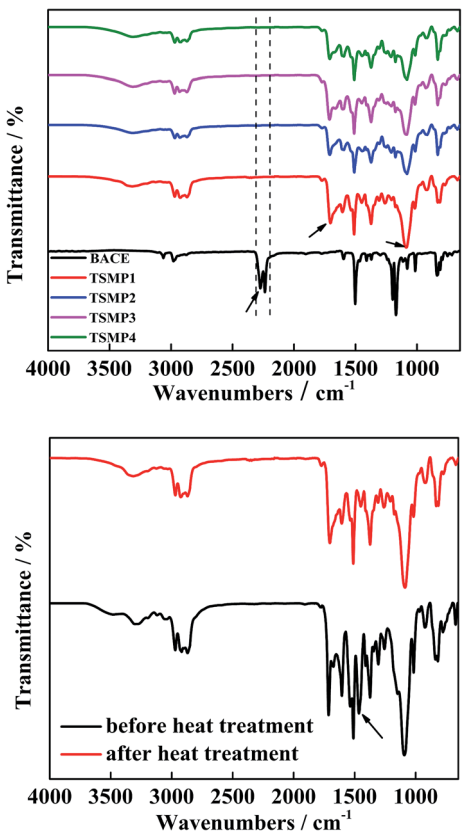

Fig. 3 FTIR spectra of (a) BMI based TSMPs with different mixture ratios and (b) TSMP1 before and after heat treatment at temperature of 200 °C.

with an extensometer at room temperature. Standard dog-bone shaped samples (ASTM D638, Type IV) for this tensile test were cut off from the polymer sheet by using a laser cutter and strained at a speed of 5 mm min^{-1}.

To characterize the dual- and triple-shape memory behaviours quantitatively, DMA Q800 (TA Instruments) was conducted under a force controlled mode by using a tensile film fixture. A schematic of the whole shape memory process is shown in Fig. 2. Each sample was heated to the temperature above its T_g with a small preload. After heat preservation for a few minutes, the sample was deformed to the expected strain *via* elevating the force. Then, the temperature was cooled down with the constant external force. When the temperature was low enough to fix the temporary shape, the external force could be removed. Finally, the sample was heated again to complete the shape memory cycle (SMC). Specimen with the dimension of 30 × 5 × 1 was utilized in this experiment. To calculate the shape fixity (R_f) and recovery ratio (R_r) during each SMC, the following equations were used:[1]

$$R_f(x \to y) = \frac{\varepsilon_y - \varepsilon_x}{\varepsilon_{y,\mathrm{load}} - \varepsilon_x} \times 100\%$$

$$R_r(x \to y) = \frac{\varepsilon_x - \varepsilon_{y,\mathrm{rec}}}{\varepsilon_x - \varepsilon_y} \times 100\%$$

here x and y represent different shapes of one sample in a shape memory cycle; "load" and "rec" indicate the strain before unloading and the strain after recovery for each shape, respectively.

The shape memory behaviors in this study were also characterized by a visual bending test. Each rectangular sample ($70 \times 5 \times 1$ mm^3) was heated to a higher temperature over its T_g. Then, the first shape was quickly realized when the sample became completely soft. For dual shape memory effect, this was the only deformation procedure during the shape memory process. For triple shape memory behavior, such deformed sample was moved into a lower temperature oven subsequently with external constraint to fix the first temporary shape. Once this procedure was finished, the sample was proceeded with the second temporary shape by external force and fixed at room temperature. The shape recovery behaviors could be observed upon reheating the sample to the deformation temperature.

Results and discussion

ATR-FTIR analysis of BMI based TSMPs chemical structure

The covalent crosslinks in the BMI based TSMPs were investigated by ATR-FTIR analysis. After the linear backbone of the BMI molecular structure formed, BACE with highly reactive cyanate functional groups was introduced into the polymeric system as a crosslinking agent. Fig. 3a shows the FTIR spectra of the

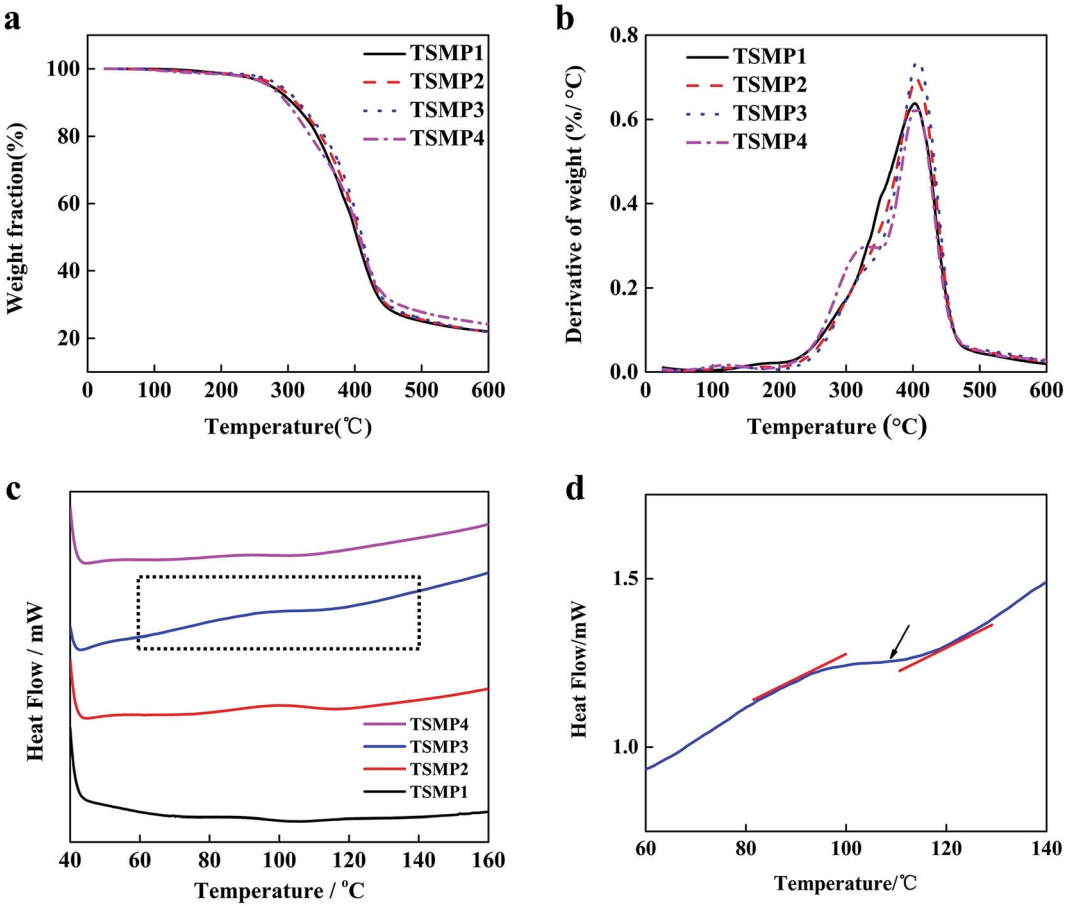

Fig. 4 Thermal performance of BMI based TSMPs: (a) TG curves; (b) DTG curves; (c) DSC curves; (d) a magnification for the selected area.

samples without thermally curing. For BMI based TSMPs, the peaks at 1709 cm^{-1} and 1175 cm^{-1} belonging to carbonyl and C–N–C (part of imine), respectively, could be observed as main characteristic peaks. When compared with the spectrum of neat BACE, it is clear that the peak at 2200–2280 cm^{-1} belonging to cyanate ester disappears completely. Meanwhile, the peak at 1560–1520 cm^{-1} corresponding to triazine ring does not exist. Such results indicate that the cyanate ester groups react with the secondary amine protons in the linear polymer chain as crosslinking agent instead of forming a triazine ring. The first kind of crosslinking points were fabricated by this reaction. In Fig. 3b, comparing to the spectrum of samples without thermally curing, the peak at 1464 cm^{-1} standing for methylene disappears after heat treatment. It indicates that further crosslinking reaction happens during the heating process, which formed another kind of crosslinking points. The complex heterogeneous crosslinking network formed in the polymeric system contributes to a broad glass transition temperature range of the polymer, which is the main reason for achieving the multiple shape memory effect.

Thermal performance analysis

Thermal stabilities of the BMI based TSMPs with different proportions were investigated by TGA in the nitrogen atmosphere from 25 °C to 600 °C at a heating rate of 10 °C min^{-1}. Fig. 4a and b show a series of thermogravimetric curves. The temperatures of minimal (<5%) decompositions (T_D) for all examined sample are above 250 °C, which are higher than T_g of the materials. It demonstrates that the BMI based TSMPs can be used durably in their operating temperature ranges without significant thermal degradation. There is just a slight decrease for TSMP4, which caused by the transport-limited reaction between secondary amines.[33] Due to the same type of chemical bonds, all the samples showed major decompositions at about 400 °C. Therefore, this approach is an appropriate method to achieve triple-shape memory ability without sacrifice of thermal stabilities of thermosetting SMPs.

The typical DSC curves of our BMI-based TSMPs samples are shown in Fig. 4c. The steps related to the glass transition process of thermosetting polymers could be seen clearly in Fig. 4d which is a magnification for the selected area in Fig. 4c. The T_g was 95.6 °C, 106.3 °C, 111.8 °C and 114.2 °C for TSMP1, TSMP2, TSMP3 and TSMP4, respectively. As expected, the T_g increases with the raising crosslinking density.

Dynamic mechanical analysis

The dynamic mechanical properties of the BMI based TSMPs during the heating process are characterized by the DMA. Fig. 5 presents the curves of storage modulus and tan δ. The stiffness of the material *versus* temperature is obtained from the storage modulus curves. All the samples present a glassy plateau at a lower temperature with high modulus and a rubbery plateau at a higher temperature with low modulus. Between the two plateaus, a sharp decline of modulus can be observed. The decrease of several orders of magnitude in the storage modulus covers a wide temperature range, which demonstrates the potential of multiple shape memory effect. Also, the storage

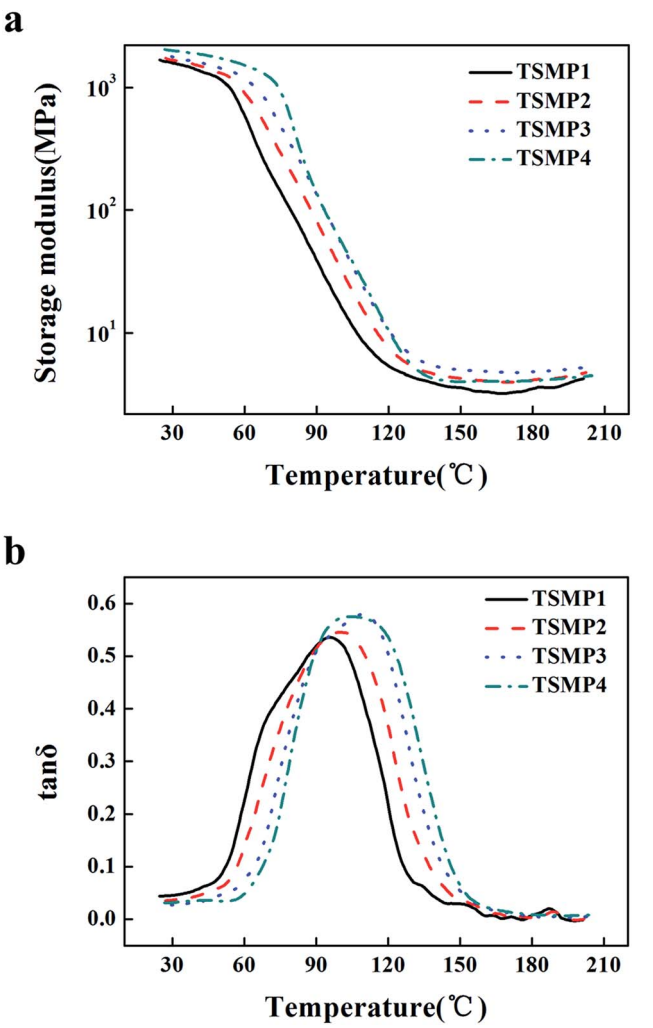

Fig. 5 DMA results in tension: (a) storage modulus (E') and (b) tan δ.

modulus at high-temperature increases with increasing amount of BACE, which is consistent with higher crosslinking density. The decrease between TSMP3 and TSMP4 could be attributed to maximum potential crosslinking density being approached at TSMP3. tan δ, using to evaluate the dissipation of energy stored in the material after elastically deformation, is defined as the relative ratio of the loss modulus to the storage modulus. In this study, we also employ the measured peak of the tan δ curve as an estimate for T_g. All the measured parameters from DMA curves are summarized in Table 2. The T_g of all the samples

Table 2 DMA properties of BMI based TSMPs[a]

Sample	E_G/MPa	E_I/MPa	E_R/MPa	T_g/°C
TSMP1	1573	924	3.66	95
TSMP2	1654	910	4.03	100
TSMP3	1755	318	4.79	120
TSMP4	1991	329	4.17	123

[a] E_G: storage modulus of glassy state (25 °C); E_I: storage modulus of intermediate state (T_g – 40 °C); E_R: storage modulus of rubbery state (T_g + 40 °C); T_g: glassy transition temperature.

determined by DMA is almost consistent with the T_g determined by DSC. However, the breadth of the glass transition temperature range has no discernible correlation with the changes in crosslinking density in BMI based TSMPs. The broader tan δ peak also indicates that the crosslinking network of BMI based TSMPs is a more heterogeneous structure.[34]

The mechanical properties of BMI based TSMPs

The mechanical properties of BMI based TSMPs at room temperature are showed in Fig. 6, including tensile stress–strain curves (Fig. 6a), tensile strength (Fig. 6b), elastic modulus (Fig. 6c) and elongation at break (Fig. 6d). The formation of chemical crosslinking structures has a significant effect on the mechanical properties of the BMI based TSMPs, especially for the influence of crosslinking density. The stress at break increases first with the increase of the crosslinking agent and then decreases rapidly due to the excessive crosslinking of the materials. The data of Young's modulus presents similar changing trend. The elongation at break, however, of the samples do display a different tendency compared with the above properties. It decreases with the increasing crosslinking density as expected. It can be attributed to the increase of crosslinking density having a negative effect on the toughness of polymers. Compared with the mechanical properties of TSMPs in previous reports,[23,24] BMI based TSMPs have a much more higher tensile strength and elastic modulus. The elongation at break is acceptable as thermosetting polymers. All these results show that the mechanical properties of BMI based TSMPs are satisfying to meet the requirements of practical applications.

Shape memory behaviour of BMI based TSMPs

For quantitatively characterizing the shape memory behavior of BMI based TSMPs, a cyclic thermo-mechanical tensile test was adopted. A typical dual shape memory cycle of this material was also shown in Fig. 7a. In the deformation process, the sample was stretched to a temporary shape with a constant force at the temperature above T_g (160 °C). Then cool the sample to the room temperature and remove the external force. The sample is fixed in the temporary shape at this moment. Finally, the sample was reheated to 160 °C to observe the recovery process. The good shape fixity ratio and recovery ratio are listed in Table 3. The result of triple shape memory behaviour of BMI based TSMPs achieved was clarified in Fig. 7b. The original shape "S0" was first stretched to 8% strain under the force of 0.6 N at 160 °C and cooled to 80 °C to obtain temporary shape "S1". Then the sample was further stretched an additional 2% strain and fixed at 25 °C to obtain temporary shape "S2". While the deformed sample was reheating to 80 °C, the temporary shape "S1" was obtained. The sample was heated to 160 °C subsequently, and its shape would change toward the original state "S0". The shape fixity and recovery ratios measured during the triple shape memory cycles (averages of three cycles) are also summarized in Table 3. Each

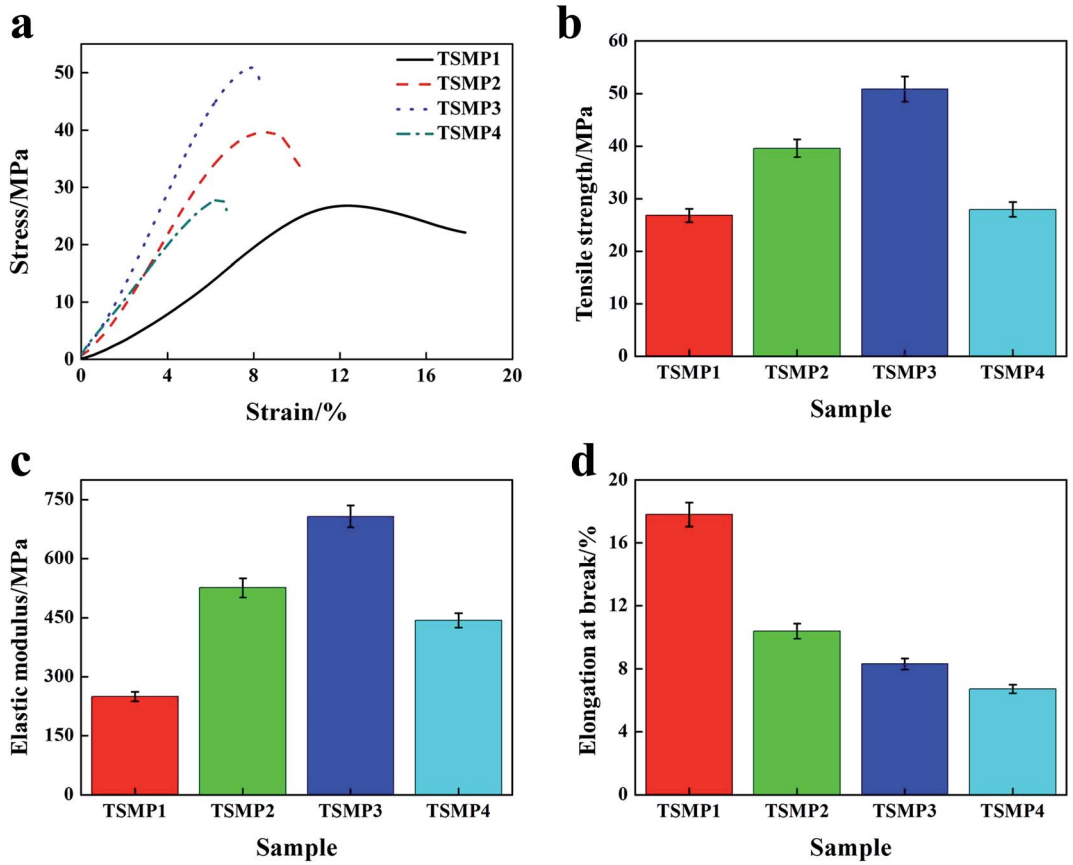

Fig. 6 Mechanical properties of BMI based TSMPs: (a) tensile stress–strain curves; (b) tensile strength; (c) elastic modulus; (d) elongation at break.

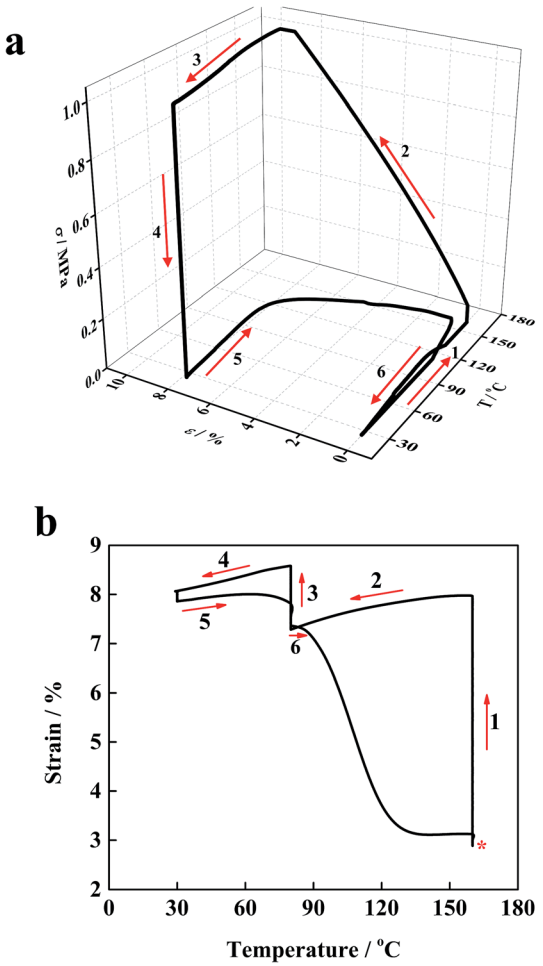

Fig. 7 (a) The triple-shape memory cycle of TSMP3. The beginning of the cycle is marked by the asterisk. The arrows denote the various stages, specifically (1) 1st deformation, (2) 1st fixing and unloading, (3) 2nd deformation, (4) 2nd fixing and unloading, and (5 and 6) recovery. (b) The dual-shape memory cycle for TSMP3. The arrows denote the various stages, specifically (1) heating, (2) deformation, (3) fixing, (4) unloading, and (5 and 6) recovery.

Table 3 Fixing and recovery ratios of BMI based TSMPs

	Dual-shape memory cycles		Triple-shape memory cycles			
Sample	R_f%	R_r%	R_f (1)%	R_f (2)%	R_r (2 → 1)%	R_r (1 → 0)%
TSMP1	99	98	98	97	98	99
TSMP2	98	100	100	95	93	97
TSMP3	100	99	100	96	92	99
TSMP4	98	98	99	97	89	100

sample performed a satisfying fixing of both temporary shape "S1" and shape "S2". The fixing of temporary shape "S2" was better for one single sample. This could be attributed to the higher storage modulus at low temperature (25 °C) compared to that at an intermediate temperature. R_r (2 → 1) and R_r (1 → 0) were also above 80% in all cases. Moreover, the molecular segmental mobility between different chemical crosslinking points was different at the same temperature, which contributed to the triple-shape memory behavior of thermoset polymer. This effect could be observed at any temperatures above the onset temperature of glass transition process. To witness this effect more apparently, we chose temperatures of $T_g \pm 40$ °C as deformation temperatures here. These two temperatures would be within the transition process due to the broad T_g range.

Demonstration of shape memory cycle of BMI based TSMPs

To demonstrate shape memory behavior of BMI-based TSMPs qualitatively, rectangular strip specimens of each sample were bended at their deformation temperatures in an isothermal oven. Two different bending methods were chosen to clarify the shape memory properties of TSMP3. For dual-shape memory effect, a series of pictures captured from the process are shown in Fig. 8a. It is clear that the sample have a good fixity for the "U" shape, and they can recover to the original shape within one minute. This process could be repeated for five times without any damage observed on the sample surface.

In terms of triple-shape memory behavior, a longer strip specimen (S0) was used to display the whole process. In this process, temporary shape (S1) was fixed at a higher temperature due to the vitrification of partial segments. Then, temporary

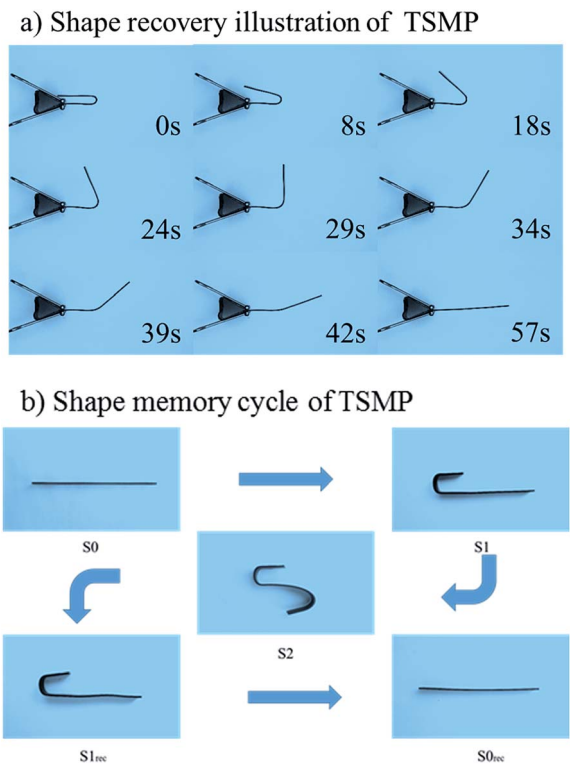

Fig. 8 Visual demonstration of shape memory properties (TSMP3): (a) recovery process of dual-shape memory behavior; (b) triple-shape memory cycle. S0: permanent shape; S1: first temporary shape (T_{d1}: 160 °C); S2: second temporary shape (T_{d2}: 80 °C); $S1_{rec}$: recovered first temporary shape (T_{r1}: 80 °C); $S0_{rec}$: recovered permanent shape (T_{r2}: 160 °C).

shape (S2) can be obtained due to the rest network vitrification at a lower temperature. The deformation temperatures we selected were consistent with the qualitative test above (Fig. 7a). A series of photos taken during the triple-shape memory cycle process of TSMP3 are shown in Fig. 8b. The left side of the sample is fixed at 80 °C (near the initial temperature of the glass transition) in image S1 and the right side of the sample is fixed at 160 °C (near the final temperature of the glass transition) in image S2. The right side of the sample recovers when the sample is heated to an intermediate temperature in image $S1_{rec}$ and the left side of the sample starts to recover, and the sample goes to its permanent, flat shape in image $S0_{rec}$.

Mechanism of triple-shape memory effects of BMI based thermosetting polymer

A typical dual-shape memory effect of thermosetting polymer with a narrow T_g range could be illustrated by a two-phase mechanism, in general, which the chemical crosslinking points are regarded as the permanent phase, and the mobile macromolecule segments are regarded as the reversible phase. In this work, we form a polymer network consisting of heterogeneous crosslinking structure to achieve triple-shape memory effect. The molecular chains between different chemical crosslinking points show differentiated responses at the same temperature in this complex network. Thus, there are more than one types of reversible phase in the polymer network which could lead to triple-shape memory effect. A simplified schematic of the visual comparison among different molecular chains is shown in Fig. 9.

Here, chain A and chain B stand for two kinds of molecular chain segments between different types of crosslinking points with different mobility. At the high temperature above T_g, both chain A and chain B are the most flexible and the material could be deformed to the first temporary shape. At a certain intermediate temperature, chain A was already relative frozen that could function to memorize the first temporary shape, while chain B still has certain mobility which was responsible for obtaining the second temporary shape. After the two-step programming process, chain A and chain B are both frozen in the second temporary shape at the temperature lower than T_g.

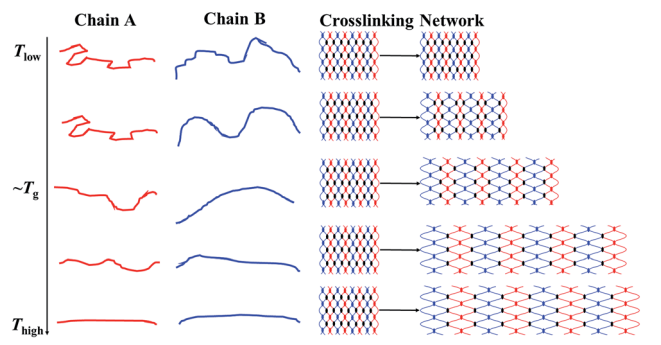

Fig. 9 A visualization of conformations for representative chain models and crosslinking network at different temperatures from T_{low} to T_{high}.

When the temperature increases to the above intermediate temperature again, chain B achieves mobility firstly while chain A is still in the frozen state. The polymer could recover to the first temporary shape. At last, chain A and chain B both achieve the maximal mobility at the temperature above T_g and the material could recover to its original shape, and the triple shape memory cycle completes. If the polymer has a more complex heterogeneous crosslinking structure than the fabricated BMI based TSMPs, the types of chain segments with different mobility are uncountable. In this situation, polymers would memorize different temporary shapes at different temperatures. Thus, the multiple shape memory materials could be obtained.

Conclusions

A series of BMI based TSMPs were successfully synthesized by adding BACE as cross-linking agent. The complex covalent crosslinked networks formed by BMI and BACE contributed to a broad range of glass transition temperature, which endowed the feasibility of triple shape memory effect. Infrared spectroscopy indicated that the complex amorphous polymer networks were formed by different types of covalent crosslinks, which the experiment results gave out a strong consistency of the proposed reactions. The crosslinking density influenced the thermal stability and mechanical properties of BMI based TSMPs. Compared to other physical approaches to obtain TSMPs, no adverse effect on these properties was found according to the test results. Triple-shape memory behavior could be achieved from all samples, where two shapes were independently recovered in response to the heat stimulus. The method taken here paves the way for the chemical process to obtain triple shape memory behavior of thermosetting polymers. The research about polymers that can memorize each temporary shape during a more complex deformation process needs to deepen more in the future.

Acknowledgements

This work is supported by the National Natural Science Foundation of China (Grant No. 11225211), for which we are very grateful.

References

1 M. Behl and A. Lendlein, *Mater. Today*, 2007, **10**, 20–28.
2 J. Leng, X. Lan, Y. Liu and S. Du, *Prog. Mater. Sci.*, 2011, **56**, 1077–1135.
3 A. Lendlein and S. Kelch, *Angew. Chem., Int. Ed.*, 2002, **41**, 2034–2057.
4 L. Yu and H. Yu, *ACS Appl. Mater. Interfaces*, 2015, **7**, 3834–3839.
5 N. G. Sahoo, S. Rana, J. W. Cho, L. Li and S. H. Chan, *Prog. Polym. Sci.*, 2010, **35**, 837–867.
6 H. Lv, J. Leng, Y. Liu and S. Du, *Adv. Eng. Mater.*, 2008, **10**, 592–595.
7 Y. Li, H. Chen, D. Liu, W. Wang, Y. Liu and S. Zhou, *ACS Appl. Mater. Interfaces*, 2015, **7**, 12988–12999.

8 D. Roy, J. N. Cambre and B. S. Sumerlin, *Prog. Polym. Sci.*, 2010, **35**, 278–301.
9 C. Liu, H. Qin and P. T. Mather, *J. Mater. Chem.*, 2007, **17**, 1543–1558.
10 M. C. Serrano, L. Carbajal and G. A. Ameer, *Adv. Mater.*, 2011, **23**, 2211–2215.
11 J. Kunzelman, T. Chung, P. T. Mather and C. Weder, *J. Mater. Chem.*, 2008, **18**, 1082–1086.
12 A. Khaldi, C. Plesse, F. Vidal and S. K. Smoukov, *Adv. Mater.*, 2015, **27**, 4418–4422.
13 J. Hu and S. Chen, *J. Mater. Chem.*, 2010, **20**, 3346–3355.
14 X. Lan, Y. Liu, H. Lv, X. Wang, J. Leng and S. Du, *Smart Mater. Struct.*, 2009, **18**, 024002.
15 W. Chen, C. Zhu and X. Gu, *J. Appl. Polym. Sci.*, 2002, **84**, 1504–1512.
16 Y. Dong, Q.-Q. Ni and Y. Fu, *Composites, Part A*, 2015, **72**, 1–10.
17 K. Yu, A. W. McClung, G. Tandon, J. Baur and H. Jerry Qi, *Mech. Time-Depend. Mater.*, 2014, **18**, 453–474.
18 F. Li, A. Perrenoud and R. C. Larock, *Polymer*, 2001, **42**, 10133–10145.
19 Q. Meng, J. Hu, L. Y. Yeung and Y. Hu, *J. Appl. Polym. Sci.*, 2009, **111**, 1156–1164.
20 K. S. Santhosh Kumar, R. Biju and C. P. Reghunadhan Nair, *React. Funct. Polym.*, 2013, **73**, 421–430.
21 L. Jinsong, W. Xuelian and L. Yanju, *Smart Mater. Struct.*, 2009, **18**, 095031.
22 T. Xie, *Nature*, 2010, **464**, 267–270.
23 R. Dolog and R. A. Weiss, *Macromolecules*, 2013, **46**, 7845–7852.
24 U. Nöchel, U. N. Kumar, K. Wang, K. Kratz, M. Behl and A. Lendlein, *Macromol. Chem. Phys.*, 2014, **215**, 2446–2456.
25 A. H. Torbati, H. B. Nejad, M. Ponce, J. P. Sutton and P. T. Mather, *Soft Matter*, 2014, **10**, 3112–3121.
26 X. Luo and P. T. Mather, *Adv. Funct. Mater.*, 2010, **20**, 2649–2656.
27 T. Xie, X. Xiao and Y.-T. Cheng, *Macromol. Rapid Commun.*, 2009, **30**, 1823–1827.
28 G. Li and W. Xu, *J. Mech. Phys. Solids*, 2011, **59**, 1231–1250.
29 G. Li, A. King, T. Xu and X. Huang, *J. Mater. Civ. Eng.*, 2013, **25**, 393–402.
30 C. P. R. Nair, *Prog. Polym. Sci.*, 2004, **29**, 401–498.
31 M. Amber, S. Joseph, B. Jeffery, R. Stephanie and M. Shawna, *presented in part at the 52nd AIAA/ASME/ASCE/AHS/ASC Structures, Structural Dynamics and Materials Conference*, Denver, April 2011.
32 Z. W. Shen, J. R. Schlup and L. T. Fan, *J. Appl. Polym. Sci.*, 1998, **69**, 1019–1027.
33 J. A. Shumaker, A. J. W. McClung and J. W. Baur, *Polymer*, 2012, **53**, 4637–4642.
34 A. R. Kannurpatti, J. W. Anseth and C. N. Bowman, *Polymer*, 1998, **39**, 2507–2513.